Kaposi's sarcoma-associated herpesvirus interacts with EphrinA2 receptor to amplify signaling essential for productive infection

Sayan Chakraborty, Mohanan Valiya Veettil, Virginie Bottero, and Bala Chandran[1]

H. M. Bligh Cancer Research Laboratories, Department of Microbiology and Immunology, Chicago Medical School, Rosalind Franklin University of Medicine and Science, North Chicago, IL 60064

Kaposi's sarcoma-associated herpesvirus (KSHV), etiologically associated with Kaposi's sarcoma, uses integrins ($\alpha3\beta1$, $\alpha V\beta3$, and $\alpha V\beta5$) and associated signaling to enter human dermal microvascular endothelial cells (HMVEC-d), an in vivo target of infection. KSHV infection activated c-Cbl, which induced the selective translocation of KSHV into lipid rafts (LRs) along with the $\alpha3\beta1$, $\alpha V\beta3$, and xCT receptors, but not $\alpha V\beta5$. LR-translocated receptors were monoubiquitinated, leading to productive macropinocytic entry, whereas non-LR–associated $\alpha V\beta5$ was polyubiquitinated, leading to clathrin-mediated entry that was targeted to lysosomes. Because the molecule(s) that integrate signal pathways and productive KSHV macropinocytosis were unknown, we immunoprecipitated KSHV-infected LR fractions with anti-$\alpha3\beta1$ antibodies and analyzed them by mass spectrometry. The tyrosine kinase EphrinA2 (EphA2), implicated in many cancers, was identified in this analysis. EphA2 was activated by KSHV. EphA2 was also associated with KSHV and integrins ($\alpha3\beta1$ and $\alpha V\beta3$) in LRs early during infection. Preincubation of virus with soluble EphA2, knockdown of EphA2 by shRNAs, or pretreatment of cells with anti-EphA2 monoclonal antibodies or tyrosine kinase inhibitor dasatinib significantly reduced KSHV entry and gene expression. EphA2 associates with c-Cbl-myosin IIA and augmented KSHV-induced Src and PI3-K signals in LRs, leading to bleb formation and macropinocytosis of KSHV. EphA2 shRNA ablated macropinocytosis-associated signaling events, virus internalization, and productive nuclear trafficking of KSHV DNA. Taken together, these studies demonstrate that the EphA2 receptor acts as a master assembly regulator of KSHV-induced signal molecules and KSHV entry in endothelial cells and suggest that the EphA2 receptor is an attractive target for controlling KSHV infection.

virus entry | productive endocytosis | receptor tyrosine kinase

Kaposi's sarcoma-associated herpesvirus (KSHV) is etiologically associated with Kaposi's sarcoma (KS), primary effusion lymphoma (PEL), and multicentric Castleman's disease (MCD) (1, 2). KSHV uses endocytosis for its entry into human endothelial cells, fibroblasts, B cells, and monocytes and uses actin-dependent macropinocytosis to enter into human microvascular dermal endothelial (HMVEC-d) cells and umbilical vein endothelial (HUVEC) cells (3). KSHV entry into adherent target cells is a multistep complex process, involving various viral glycoproteins and multiple cell surface molecules, which overlaps with the induction of host preexisting signal molecules followed by entry into the cytoplasm, release of viral capsid, and transport toward the nucleus via dynein-mediated transport along the acetylated thickened bundles of microtubules (3).

Our present studies are focused on HMVEC-d cells, one of KSHV's natural in vivo target cells. KSHV attachment to the HMVEC-d cell surface occurs via heparan sulfate (HS) followed by temporal interactions with integrins ($\alpha3\beta1$, $\alpha V\beta3$, and $\alpha V\beta5$) and the transporter xCT molecule. KSHV binding to these molecules results in the induction of FAK, Src, PI3-K, Rho-GTPases, Dia-2, PKC-ζ, ERK1/2, and NF-κB signal molecules (3–8). Our studies using chemical inhibitors, dominant negative proteins, or cells lacking these molecules have shown that FAK, Src, PI3-K, and RhoA activation is necessary for KSHV entry (3–8). Microtubule acetylation by RhoA-GTPase induces the Diaphanous-2 molecule that facilitates the transport of capsid toward the nucleus via dynein motors (3–8). KSHV-induced ERK and NF-κB are essential for the initiation of viral gene expression. Disruption of HMVEC-d cell lipid rafts (LRs) by MβCD results in increased Src activation and virus entry. However, MβCD inhibits PI3K, RhoA, Dia-2, and NFκB activation; microtubule acetylation; nuclear delivery of viral DNA; and viral gene expression (3–9). Nuclear delivery of KSHV genomic DNA does not lead to lytic gene expression and progeny virus formation; instead, KSHV expresses its latent genes and establishes latency (3). Hence expression of latency-associated genes is used as an indicator of infection and to monitor the effects of inhibition of various molecules involved in infection.

Although macropinocytosis is used by many viruses (10), the identity of the molecule(s) mediating macropinosome formation, entry, and mechanisms is not known. Our studies revealed that KSHV exploited c-Cbl, an E3 ubiquitin ligase, to enter endothelial cells via bleb-induced macropinocytosis (11). Mass spectrometric analyses disclosed that the interaction of c-Cbl with myosin IIA was also essential for macropinocytosis. Our subsequent studies on determining the link between KSHV receptors, c-Cbl, and LRs revealed that very early during infection [1 min postinfection (p.i.)], c-Cbl induced the selective translocation of KSHV into the LR along with $\alpha3\beta1$, $\alpha V\beta3$, and xCT receptors, but not $\alpha V\beta5$. Activated c-Cbl localized with LRs at the junctional base of macropinocytic blebs. LR-translocated receptors were monoubiquitinated, leading to productive macropinocytic entry, whereas non-LR–associated $\alpha V\beta5$ was polyubiquitinated, leading to clathrin-mediated entry that was targeted to lysosomes. c-Cbl knockdown blocked macropinocytosis and receptor translocation and diverted KSHV to a clathrin–lysosomal noninfectious pathway. Similar results were also seen by LR disruption (12).

Our studies revealed that KSHV's interactions with the HMVEC-d cell surface progress into a complex event and demonstrated that c-Cbl regulates macropinocytic entry by differential ubiquitination and translocation of selected KSHV receptors into LRs. However, the identities of molecules that recruit c-Cbl and integrate signal pathways to mediate KSHV entry into HMVEC-d

cells and the mechanism by which interaction of KSHV with integrins and subsequent induction of host cell signaling that leads to productive virus endocytosis are not known. To determine this process, we immunoprecipitated the LR fractions from HMVEC-d cells infected with KSHV for 5 min with anti-integrin α3β1 antibody and analyzed them by mass spectrometry. The transmembrane 134-kDa EphrinA2 (EphA2) receptor was one of the proteins identified in this analysis.

The Eph family of receptor tyrosine kinases (RTK) and their membrane-tethered ligands, known as Ephrins, constitute the largest RTK subfamily, with at least 14 receptors and nine ligands (13). EphA2 binds to membrane-bound Ephrin-A ligands to exert bidirectional signaling and has broad implications in many cancers (14, 15). Together with integrin-associated signaling, Ephrins and Eph receptors mediate diverse activities such as effects on the actin cytoskeleton, cell–substrate adhesion, intercellular junctions, cell shape, and cell movement (16–19). Ephrins and Eph receptors modulate the endothelial cellular assembly by controlling various signaling pathways (20). Ephrin receptors have also been shown to be the center of signaling crosstalk between integrins, PI3-K, and Rho-GTPases (21, 22), which are also induced during KSHV infection (3).

In this report, we demonstrate that KSHV interacts with EphA2, which regulates KSHV endothelial cell entry by coordinating integrin-associated signaling and macropinocytic events.

Results

Integrin α3β1 Associates with LR-Associated EphA2 Early During KSHV Infection of HMVEC-d Cells. Our earlier studies revealed a unique c-Cbl–mediated translocation of selective KSHV entry receptors (α3β1, αVβ3, and xCT) into LRs of HMVEC-d cells that is followed by macropinocytic entry and latent infection (12). To identify the potential cell surface molecules involved in assembling integrin-associated signal molecules, HMVEC-d cells were infected with KSHV (10 DNA copies per cell) for 5 min, and LR fractions from uninfected and infected cells were isolated, immunoprecipitated with anti-α3β1 antibodies, and analyzed by mass spectrometry [liquid chromatography (LC)-MS/MS]. Analysis identified several proteins such as myosin IIA, integrin β1, EphA2, Hsp90, calnexin, fibrinopeptide subunit B, actin, and proteasome 26S proteins both in the uninfected and in the KSHV-infected LR immunoprecipitates (Table S1 and Fig. S1A). However, compared with uninfected LRs, we observed an enriched association of these identified molecules in the infected LR fractions (Fig. S1A). We validated the mass-spectrometry data with coimmunoprecipitation experiments with anti-α3β1 antibodies. As shown in Fig. S1B, these results confirmed the increased association of myosin IIA, Hsp90, calnexin, and proteasome 26s with integrin α3β1 at 5 min p.i. These results suggested a minimal association of the identified proteins with integrin α3β1 in uninfected LR samples that were increased by KSHV infection (Fig. S1 A and B), which could be due to rapid translocation of KSHV receptor (α3β1, αVβ3, and xCT) into the infected cell LRs as shown by our earlier studies (12). In addition, detection of actin and myosin IIA as α3β1-associated LR proteins (Table S1 and Fig. S1 A and B) also supported our previous finding that actin–myosin interaction is required for macropinocytic entry of KSHV (11).

Among the molecules identified, we considered EphA2 as an attractive candidate for recruitment and assembly of KSHV-induced signal molecules in HMVEC-d cells because of its cell-surface expression and LR localization (23, 24). To ascertain the role of the identified EphA2 during KSHV infection, we first tested the localization of EphA2 in LRs, as suggested by our LC/MS-MS results. LR fractionation analysis revealed that EphA2 partitioned into LRs in uninfected and KSHV-infected HMVEC-d cells (Fig. 1A) and not in the non-LR fractions.

KSHV Activates EphA2 Early During Infection of HMVEC-d Cells. Ephrin receptors are activated by phosphorylation, a key step for receptor signaling and internalization (25, 26). To determine whether KSHV infection activated EphA2, we examined the localization of phosphorylated EphA2 by immunofluorescence assays. Compared with the diffuse and scattered detection pattern of phospho-EphA2 (pEphA2) in uninfected cells, at 10 min p.i., we observed that pEphA2 colocalized with the cell surface LR marker flotillin-1 (Fig. 1B, Top Right and Middle Right, Insets). This aggregation of an LR marker has been shown to be induced by KSHV early during infection (12). At 30 min p.i., the majority of pEphA2s localized to the clustered LRs appeared to be internalized along with flotillin (Fig. 1B, Bottom Right, Inset). We also analyzed the uninfected or KSHV-infected HMVEC-d cells by Western blots for pEphA2. Indeed, we observed increased pEphA2 levels within 1 min p.i. (2.7-fold), which was sustained during the observed 30 min p.i. (3.2-fold) (Fig. 1C, a). Preincubation of KSHV with heparin, which inhibits virus binding, significantly reduced the pEphA2 levels (Fig. 1C, b), which demonstrated the specificity of KSHV-induced EphA2 activation.

EphA2 Coimmunoprecipitates with KSHV Entry Receptors Early During Infection of HMVEC-d Cells. To determine whether EphA2 is a key host factor associated with integrin receptors during infection, we immunoprecipitated uninfected and KSHV-infected HMVEC-d cell lysates with different integrin antibodies and Western blotted for EphA2. As reported before (27), a minimal interaction of EphA2 with integrin α3β1 was observed in uninfected cells (Fig. 1D, a, Top). In contrast, KSHV infection increased the EphA2-integrin α3β1 association, which maximized within 5 min p.i., reduced by 10 min p.i., and increased by 30 min p.i. (Fig. 1D, a, Top). We also observed coimmunoprecipitation (co-IP) of EphA2 with integrin αVβ3, following a similar pattern to that of α3β1 (Fig. 1D, a, third row). We did not observe an integrin αVβ5 association with LR resident EphA2 molecules (Fig. 1D, a, fifth row), which supports our earlier observation that during KSHV infection, integrin αVβ5 does not translocate into LRs and remains in the non-LR portion of the membrane (12). Total integrin protein levels indicated equal loading (Fig. 1D, a). We observed reduced interaction of integrin αVβ3 with EphA2 in heparin-treated KSHV-infected cells, which not only demonstrated the specificity but also suggested that virus binding is essential for EphA2 association with integrins (Fig. 1D, b). Because α3β1 and αVβ3 translocated into LRs during KSHV infection (12), we verified that EphA2 associated with the translocated integrins in LRs. Compared with non-LR fractions, at 5 min p.i., the association of integrins α3β1 and αVβ3 with EphA2 was solely observed in the LR fractions (Fig. 1D, c).

To demonstrate that KSHV infection was required for EphA2 to interact with integrins, we transfected HEK293T cells with EphA2-Myc plasmid. Compared with uninfected and GFP-Myc–transfected KSHV-infected cells, integrins α3β1 and αVβ3 associated with EphA2 only in KSHV-infected cells (Fig. 1E), which suggested that KSHV infection facilitated the association of EphA2 with integrins.

EphA2 Colocalizes with KSHV and Integrins Early During Infection of HMVEC-d Cells. To analyze whether the association of EphA2 with integrins occurs at the cell surface, mock or KSHV-infected HMVEC-d cells were immunostained with anti-EphA2 and integrin αVβ3 and α3β1 antibodies. Strong colocalization of EphA2 with integrins αVβ3 and α3β1 was observed at the edges of infected cells (Fig. 2 A and B). Compared with uninfected cells, line scan analysis on the enlarged KSHV-infected cells depicted a coherent signal intensity pattern between EphA2 and integrins αVβ3 and α3β1, confirming that colocalization occurred predominantly at the cell surface (Fig. 2 A and B). Compared with uninfected cells, mean pixel intensities of colocalization between integrins and EphA2 were significantly higher in KSHV-infected
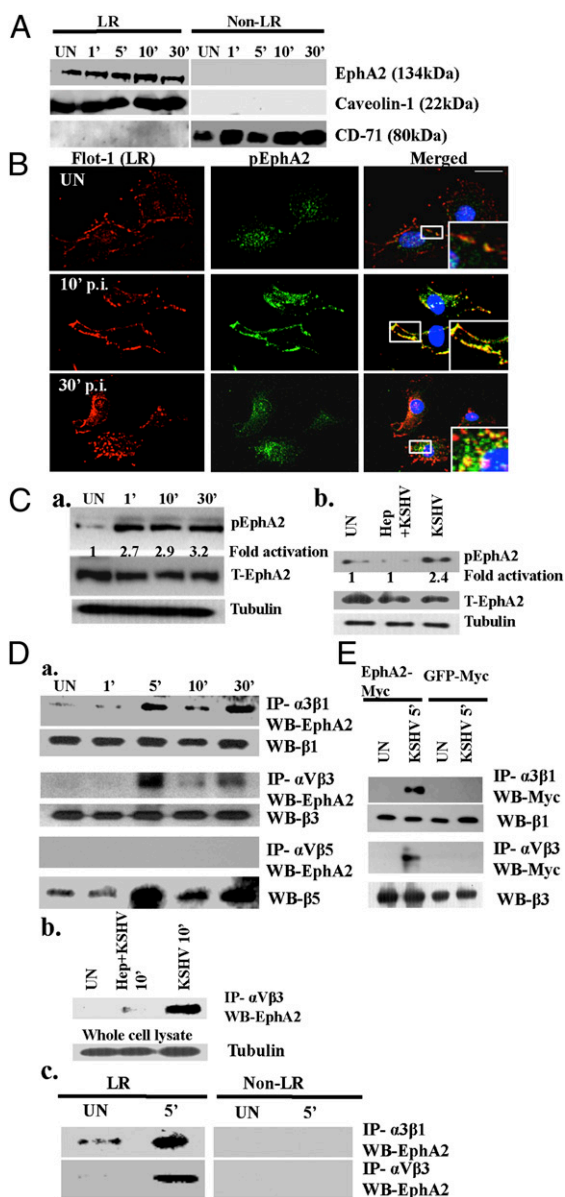
Fig. 1. Identification of EphA2 as an integrin-interacting molecule early during KSHV infection. (*A*) Serum-starved HMVEC-d cells were either mock or KSHV (10 DNA copies per cell) infected at the indicated time points. LR and non-LR fractions were isolated and analyzed for EphA2 by Western blot. Caveolin-1 and CD71 characterize the purity of LR and non-LR fractions, respectively. (*B*) Serum-starved HMVEC-d cells were either mock or KSHV infected at the indicated time points, washed, and reacted with anti-Flot-1 (LR marker) and pEphA2 antibodies, followed by Alexa 594 and 488 secondary antibodies, respectively. Representative immunofluorescence images are shown. *Insets* show the enlarged images of the boxed areas. (Scale bar: 10 μm.) (*C*, *a* and *b*) Serum-starved HMVEC-d cells were either uninfected or infected with KSHV or KSHV preincubated with 100 μg heparin for 1 h at 37 °C, for the indicated time points, and subjected to Western blot analysis for phospho-EphA2 (pEphA2). The blot was then stripped and reprobed for total EphA2 and tubulin as a loading control. (*D*) (*a*) Serum-starved HMVEC-d cells were either left uninfected or infected with KSHV for the indicated time points and immunoprecipitated with anti-α3β1, -αVβ3, or -αVβ5 antibodies and analyzed for EphA2 by Western blot. The blots were stripped and reprobed for total β1, β3, and β5, respectively. (*b*) Serum-starved HMVEC-d cells were either left uninfected or infected with heparin-treated KSHV for 10 min, immunoprecipitated with anti-αVβ3, and then Western blotted for EphA2. As loading controls, 10 μg whole-cell lysate protein was analyzed for tubulin by Western blot. (*c*) A total of 150 μg of LR and non-LR fractions from uninfected and KSHV-infected cells was immunoprecipitated with anti-

cells (Fig. 2*C*, *P* = 0.00016). There was no change in the levels of integrins β1 and β3 after 10 min p.i., further confirming that KSHV induced a rearrangement of integrins at the cell surface LRs without increasing their total protein levels (Fig. S2). In contrast, EphrinB2 (EphB2), a class-B Ephrin receptor, did not show any increased colocalization with integrin α3β1 in infected cells compared with uninfected cells (Fig. S3), which demonstrated the specificity of KSHV interactions with EphA2. At 10 min p.i., we also observed the colocalization of EphA2 with KSHV as detected by envelope glycoprotein gpK8.1A (Fig. 2*D*). This result also confirmed that EphA2 associates with KSHV and its entry receptors during infection.

EphA2 shRNA Inhibits KSHV Entry and Infection of HMVEC-d Cells. To characterize the functional effect of EphA2 on KSHV infection, we tested five different EphA2 lentivirus-encoding shRNAs to determine the knockdown of EphA2 levels in HMVEC-d cells (Fig. 3*A*). EphA2 shRNAs 3 and 4, which showed maximal knockdown of protein levels, were used in subsequent experiments (Fig. 3*A*). The EphA2-specific shRNAs did not have any off-target effects on common cellular signaling molecules implicated in KSHV infection (Fig. S4*A*).

Because binding to target cells is the first step in viral entry, we assessed the role of EphA2 in KSHV binding and entry. EphA2 shRNAs did not affect KSHV binding in HMVEC-d cells (Fig. 3*B*). In contrast, compared with control shRNA, EphA2 shRNAs did inhibit KSHV entry into HMVEC-d cells as determined by measuring the internalized KSHV viral (ORF73) DNA copies (Fig. 3*C*). EphA2 shRNAs 3 and 4 significantly reduced KSHV entry by 45% and 63%, respectively, compared with 19% inhibition with EphB2 shRNA (Fig. 3*C* and Fig. S4*B*). This inhibition of KSHV entry was consistent with the level of EphA2 knockdown by different shRNAs (Fig. 3*A*). Preincubation of KSHV with soluble EphA2 (SolEphA2) also resulted in a 63% inhibition of KSHV entry (Fig. 3*D*). Compared with 27,000 KSHV DNA copies in control shRNA-transduced cells, only ~9,990 KSHV DNA copies were internalized in the presence of soluble EphA2. Treatment of HMVEC-d cells with anti-EphA2 monoclonal antibodies before infection significantly blocked KSHV entry by 50%, whereas anti-EphB2 antibodies showed inhibition of only ~17% (Fig. 3*E*).

To further establish a functional role for receptor tyrosine kinases during KSHV entry, we used dasatinib, a clinically approved tyrosine kinase EphA2 inhibitor (28). Compared with DMSO control, 1 μM and 5 μM dasatinib not only inhibited EphA2 phosphorylation (by 75%) at 10 min p.i. (Fig. S4*C*), but also blocked KSHV entry by 69% and 77%, respectively (Fig. 3*F*). These results clearly demonstrated that EphA2 plays a role in KSHV entry in HMVEC-d cells.

We next determined the effect of EphA2 shRNA on KSHV latent gene expression. Control and EphA2 shRNA-transduced HMVEC-d cells were infected with KSHV for 24 h and viral gene expression was determined by real-time RT-PCR. Compared with control cells, EphA2 shRNA-3–transduced cells showed ~78% inhibition of latency-associated ORF73 gene expression (Fig. 3*G*). We did not detect ORF73 expression in EphA2 shRNA-4–transduced cells (Fig. 3*G*). Compared with control shRNA, at 48 h p.i., we observed total inhibition in nuclear LANA-1

αVβ3 or -α3β1 antibodies for 2 h at 4 °C and analyzed by Western blots for EphA2. (*E*) HEK293T cells were transfected with either EphA2-Myc or GFP-Myc plasmids. Forty-eight hours posttransfection, cells were either mock or KSHV infected (10 DNA copies per cell) and immunoprecipitated with anti-α3β1 and -αVβ3 antibodies. The immunoprecipitates were analyzed by Western blot for Myc. They were stripped and reprobed for total β1 and β3, respectively.
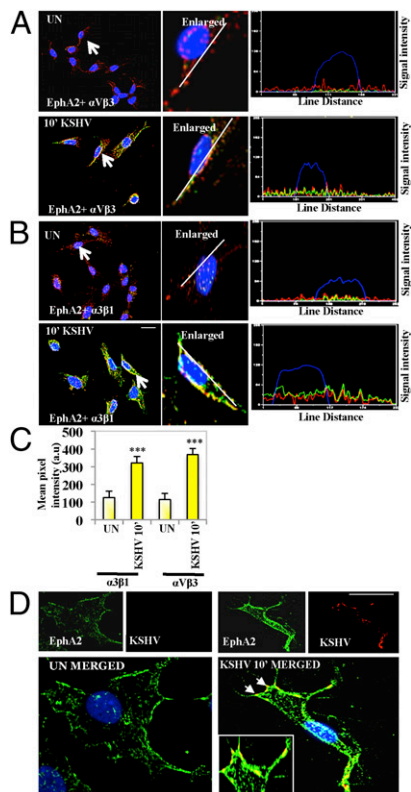
Fig. 2. Colocalization of EphA2 with integrins and KSHV during infection. (*A* and *B*) Serum-starved (8 h) HMVEC-d cells were either left uninfected or infected for 10 min with KSHV (10 DNA copies per cell), washed, and processed for immunofluorescence using rabbit anti-EphA2 and mouse anti-α3β1 or -αVβ3 antibodies for 1 h at 37 °C. Subsequently, cells were stained with either anti-rabbit Alexa fluor 594 or anti-mouse Alexa fluor 488. Arrows indicate the enlarged cell. The line-scan signal intensity analysis of the cell shown in the enlarged images on the *Right* is depicted in the *Bottom Right*. (*C*) Colocalization mean pixel intensity plot (in arbitrary units) between integrins and EphA2 at 10 min p.i. (***P = 0.00016). (*D*) Serum-starved (8 h) HMVEC-d cells were either left uninfected (UN) or infected for 10 min with KSHV (10 DNA copies per cell), washed, and processed for immunofluorescence, using mouse anti-gpK8.1A and rabbit anti-EphA2 antibodies followed by anti-mouse Alexa fluor 488 or anti-rabbit Alexa fluor 594. Representative deconvoluted images are shown. The arrows represent colocalization, which is also shown in the *Inset* as the enlarged image. (Scale bar: 10 μm.)

immunostaining in EphA2 shRNA-4–transduced cells (Fig. 3*H*). Taken together, these results suggested that EphA2 is required for establishing KSHV gene expression in HMVEC-d cells.

EphA2 Recruits a Macropinosome Complex Composed of c-Cbl, Integrin, and Myosin IIA Early During KSHV Infection of HMVEC-d Cells. Our previous studies have elucidated the requirement of c-Cbl for macropinocytosis of KSHV (11). To examine whether EphA2 regulated c-Cbl–mediated KSHV macropinocytosis and thereby KSHV entry, we first deciphered whether EphA2 interacted with c-Cbl during infection. HMVEC-d cells were either mock or KSHV infected, immunoprecipitated with anti-c-Cbl antibody, and Western blotted for EphA2. c-Cbl was associated with EphA2 as early as 1 min p.i., maximized by 10 min, and detected even at 30 min p.i. (Fig. 4*A*). Total c-Cbl levels indicated the equal loading of protein (Fig. 4*A*). During macropinocytosis of KSHV, integrin α3β1 was associated with c-Cbl in LRs of HMVEC-d cells (12). Because EphA2 associated with integrins during infection, we examined the formation of the EphA2-c-Cbl–integrin complex. When we performed a triple immunofluorescence analysis involving integrins, c-Cbl, and EphA2, we

observed that the α3β1 integrin, c-Cbl, and EphA2 complex colocalized in characteristic discrete patches at the peripheral edges of KSHV-infected cells, (Fig. 4*B*). Our high-resolution images clearly indicated that EphA2 formed a signaling complex composed of integrins and c-Cbl required for productive macropinocytic KSHV entry in HMVEC-d cells.

Our mass spectrometry data revealed the presence of myosin IIA (Table S1 and Fig. S1*B*), which we have earlier shown to interact with c-Cbl to regulate KSHV-induced macropinocytic blebs (11). To determine whether EphA2 associates with myosin IIA to regulate KSHV macropinocytosis, EphA2 immunoprecipitates were Western blotted for myosin IIA. We observed a robust association between EphA2 and myosin IIA during KSHV infection, maximizing at 10 min p.i. and that was subsequently detected at 30 min p.i., albeit at a reduced level (Fig. 4*C*). This association was further confirmed by the colocalization of EphA2 with p-myosin IIA and flotillin-1 (LR marker) early during KSHV infection of HMVEC-d cells (Fig. 4*D*).

To further validate the role of EphA2 in regulating molecular partners involved in KSHV macropinocytosis, control and EphA2 shRNA-transduced HMVEC-d cells were infected with KSHV and Western blotted for p-c-Cbl and p-myosin IIA. Compared with control shRNA cells, EphA2 shRNA (3 and 4)-transduced KSHV-infected cells showed significant reduction (70–92%) in the phosphorylation of c-Cbl at tyrosine 731 (Fig. 4*E*). A similar reduction in the activation of p-myosin IIA was observed in EphA2 shRNA-transduced cells (Fig. 4*E*). These results were further validated by the strong reduction of colocalization between p-myosin IIA and p-c-Cbl in EphA2 shRNA-transduced cells (Fig. S5 *A* and *B*). Taken together, these studies strongly suggested that EphA2 is involved in regulating molecules involved in KSHV macropinocytosis.

EphA2 Recruits the KSHV-Induced Signaling Complex into Lipid Rafts Early During Infection of HMVEC-d Cells. Because EphA2 significantly affected KSHV entry, we next determined the underlying signaling mechanism controlled by EphA2. Interaction of KSHV with integrins activates preexisting host signal molecules, such as FAK, Src, and PI3-K, which are known to regulate endocytosis (3). Furthermore, our data revealed that EphA2 modulates c-Cbl phosphorylation at tyrosine 731. Reports suggest that c-Cbl tyrosine 731 phosphorylation is dependent on PI3-K signaling (29). Therefore, to elucidate whether EphA2 interacts with Src and PI3-K induced by KSHV, we immunoprecipitated uninfected or KSHV-infected HMVEC-d cell lysates with anti-Src or EphA2 antibodies. EphA2 was coimmunoprecipitated with Src in uninfected cells; however, KSHV infection increased the association as early as 1 min p.i. and persisted during the observed 30 min p.i. (Fig. 5*A*). PI3-K-p85 was also coimmunoprecipitated with EphA2 early during infection from 1 min, which persisted during the observed 30-min period p.i. (Fig. 5*A*). High-resolution immunofluorescence images also demonstrated the association of EphA2 with Src and PI3-K, which was observed predominantly at the peripheral edges of infected cells (Fig. 5 *B* and *C* and Fig. S6 *A* and *B*). Coherent signal intensity patterns between pSrc (green), pPI3-K (green), and EphA2 (red) further confirmed that early during infection, EphA2 formed a signaling complex with KSHV-induced Src and PI3-K at the edges of infected cells.

Because LRs are a signaling hub for c-Cbl–mediated KSHV receptors and macropinocytosis (12), we tested the presence of KSHV-induced signaling in LRs. Our results demonstrated that KSHV-induced pFAK was non-LR associated and did not translocate into LRs during infection (Fig. 5*D*). Despite minimal LR localization in uninfected cells, KSHV infection promoted considerable influx of pSrc and pPI3-K in LRs as early as 1 min p.i. and 10 min p.i., which persisted during the observed 30-min period p.i., with the concomitant reduction in non-LR fractions (Fig. 5*D*). Caveolin-1 and CD-71, markers for LR and non-LR
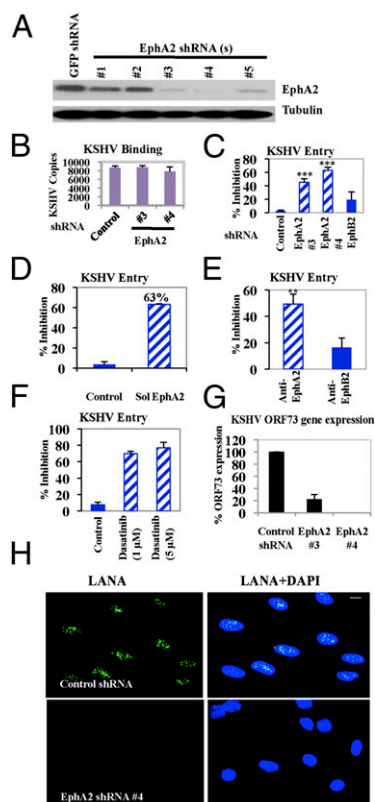
Fig. 3. Effect of EphA2 shRNA on KSHV entry and infection. (*A*) HMVEC-d cells were transduced with sh-GFP (control) or different sh-EphA2–expressing lentiviral vectors for 1 d. Cells cultured for 2 d were harvested and analyzed by Western blot for EphA2. (*B* and *C*) Control, EphA2 shRNA(s)-, or EphB2 shRNA-transduced HMVEC-d cells were infected with KSHV for 1 h at 4 °C (*B*) or 37 °C (*C*). After washing, total DNA was isolated and KSHV binding and entry were determined by real-time DNA PCR for the ORF73 gene. Each reaction was done in triplicate and each bar represents the average ± SD of three independent experiments. For *B*, results are presented as KSHV DNA copies bound to sh-EphA2–transduced and –untransduced cells. For *C*, results are presented as percentage of inhibition of KSHV DNA internalization by sh-EphA2 or EphB2 compared with untransduced cells incubated with the virus alone. (***P = 0.0001). (*D*) Untreated KSHV or KSHV preincubated with soluble EphA2 (Sol-EphA2) for 1 h at 37 °C was used to infect HMVEC-d cells for 1 h at 37 °C. Postwashing, KSHV entry was determined as described above. Each reaction was done in triplicate and each bar represents the average ± SD of three experiments. Data are presented as percentage of inhibition of KSHV DNA internalization by Sol-EphA2 compared with cells incubated with the virus alone. (*E*) HMVEC-d cells were treated with 10 μg/mL rabbit IgG, rabbit anti-EphA2, or anti-EphB2 antibodies for 1 h at 4 °C. After washing, cells were infected for 1 h at 37 °C and KSHV entry was determined as described previously. Data are represented as percentage of inhibition by Eph antibodies compared with IgG control. (**P = 0.005). (*F*) HMVEC-d cells were either left untreated or pretreated with solvent control or the indicated concentrations of dasatinib for 1 h at 37 °C. Cells were washed and infected with KSHV for 1 h at 37 °C and entry was determined. Data are represented as percentage of inhibition of KSHV DNA internalization compared with untreated cells. (*G*) Control or EphA2 shRNA-transduced HMVEC-d cells were infected with KSHV. At 24 h p.i., cells were harvested, total RNA was isolated, and viral gene expression was determined by real-time RT-PCR with KSHV ORF73 gene-specific primers. (*H*) Control or EphA2 shRNA (4)-transduced HMVEC-d cells were mock or KSHV (10 DNA copies per cell) infected for 2 h at 37 °C, washed, and cultured in complete media for another 46 h. After washing, cells were fixed and processed for immunofluorescence, using rabbit anti-LANA antibody. Representative images are shown. (Scale bar: 10 μm.)

fractions, respectively, show the purity of the fractions (Fig. 5*D*). Western blot analyses of signal molecules using whole-cell lysates (WCL) demonstrated the equal loading of proteins as well as the

lack of change in the protein levels (Fig. 5*D*). These results suggested that increased levels of pSrc and pPI3-K, but not FAK signaling were recruited and enriched in the LRs of KSHV-infected cells.

EphA2 shRNA Reduced the Activation and LR Recruitment of KSHV-Induced Signaling Molecules. To ascertain the role of EphA2 in the selective signaling amplification of Src and PI3-K in LRs of infected cells, we first determined the effect of EphA2 shRNA on the activation of KSHV-induced signaling. HMVEC-d cells transduced with control or EphA2 shRNAs were infected with KSHV for 10 min and analyzed by Western blots for different signal molecules. As expected, EphA2 knockdown did not affect pFAK levels owing to its non-LR association (Fig. 5*E*). In contrast, knocking down EphA2 reduced the activation of pSrc and pPI3-K in KSHV-infected cells by >50% (Fig. 5*E*). This reduced signaling activation by EphA2 shRNA could be the potential reason for the dramatic reduction in KSHV entry and infection in EphA2 shRNA-transduced cells, which further suggested the importance of EphA2 in KSHV infection.

Next, we tested whether EphA2 recruited and amplified KSHV-induced signaling in LRs. Accordingly, LR localization of KSHV-induced signal molecules was analyzed in control and EphA2 shRNA-transduced cells. In control shRNA-transduced and KSHV-infected cells at 10 min p.i, compared with non-LR fractions, increased pSrc, pPI3-K, and pc-Cbl were associated with LR fractions (Fig. 5*F*). In contrast, this association and enrichment of pSrc, pPI3-K, and pc-Cbl in LRs were markedly inhibited in EphA2 shRNA-4–transduced and KSHV-infected cells with a concomitant increase in non-LR fractions (Fig. 5*F*). This result suggested that EphA2 regulated the augmented activation and influx of these activated signal molecules into LRs (Fig. 5*F*). No detectable changes in the levels of total signal molecules were observed between control and EphA2 shRNA-transduced cells. Total signal molecules in the WCL did not show any marked changes (Fig. 5*F*). These studies suggested that KSHV/integrin interactions with EphA2 in LRs are critical for the amplification of Src and PI3-K activity of infected cells.

The LR clustering effect is specifically induced by KSHV–receptor translocations and associated signaling (12). Hence, we next determined whether EphA2 affected the KSHV translocations in LRs critical for integrin signaling amplification. Compared with control shRNA-transduced cells, we observed a marked reduction in the association of KSHV (gpK8.1A) in LRs of EphA2 shRNA-transduced cells (Fig. S6*C*). This observation further confirmed that EphA2 regulated c-Cbl–mediated KSHV–receptor translocations leading to LR clustering and signal amplifications.

EphA2 Regulates Productive Macropinocytosis of KSHV in HMVEC-d Cells. Our studies above demonstrated that knocking down EphA2 reduced KSHV-induced signaling, virus entry, and viral gene expression. KSHV-induced signaling is highly coupled to its endocytosis and our previous studies have demonstrated that KSHV enters HMVEC-d cells via macropinocytosis (11, 30). Evidence of associations with c-Cbl, myosin IIA, and regulation of KSHV-induced signaling prompted us to examine EphA2's role in macropinocytosis of KSHV. To determine whether EphA2 associates with macropinocytic blebs, we performed immunofluorescence assays combined with differential interference contrast (DIC) microscopy. Compared with the diffused localization in uninfected cells, pEphA2 levels were robust and clustered at the cell surface of KSHV-infected cells (Fig. 6*A*). In addition, KSHV infection promoted the protrusions of membrane blebs and pEphA2 was localized in the proximity of KSHV-induced membrane blebs (Fig. 6*A*). This result suggested a potential role of EphA2 in macropinocytosis-based internalization of KSHV. Such aggregation of EphA2 at the cell surface
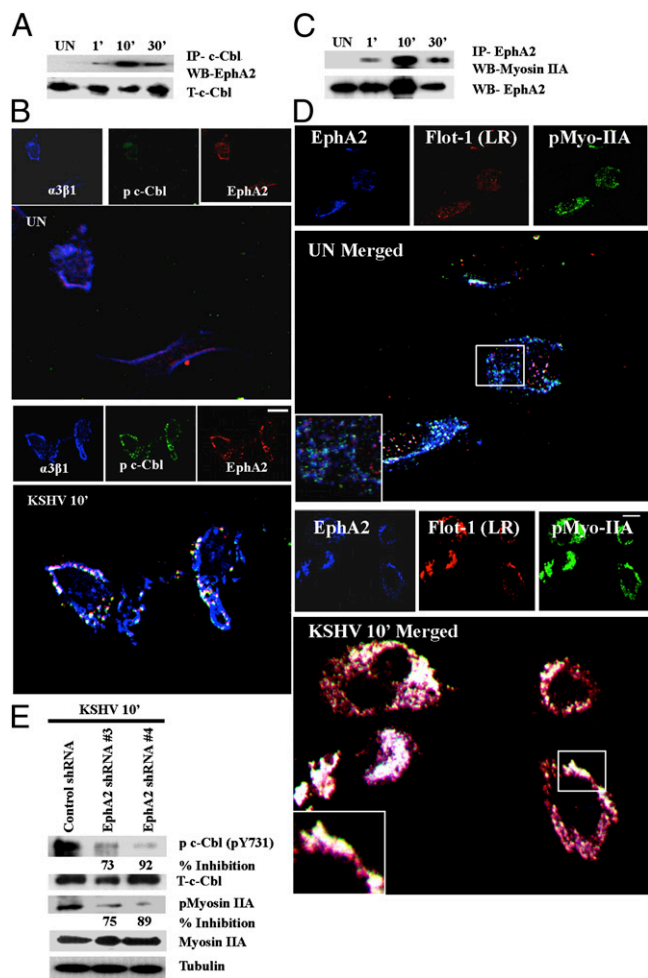
Fig. 4. KSHV-recruited EphA2 induced the formation of a c-Cbl, integrin, and myosin internalization complex. (*A*) Serum-starved HMVEC-d cells were either left uninfected or KSHV infected for the indicated time points and immunoprecipitated with anti–c-Cbl antibody and analyzed for EphA2 by Western blot. (*B*) Serum-starved (8 h) HMVEC-d cells were either left uninfected (UN) or infected for 10 min with KSHV (10 DNA copies per cell), washed, and processed for immunofluorescence assay using goat anti-EphA2, mouse anti-α3β1, and rabbit anti–c-Cbl antibodies for 1 h at 37 °C. Subsequently, cells were stained with anti-mouse Alexa fluor 405, anti-goat Alexa fluor 594, and anti-rabbit Alexa fluor 488, respectively. Representative 2D deconvoluted images are shown. (Scale bar: 10 μm.) (*C*) Serum-starved HMVEC-d cells were either uninfected or KSHV infected for the indicated time points, immunoprecipitated with EphA2 antibody, and Western blotted for myosin IIA. The blot was stripped and reprobed for EphA2. (*D*) Serum-starved uninfected (UN) or KSHV-infected HMVEC-d cells were processed as in *C* and immunostained for EphA2, p-myosin IIA, and LR marker (Flotillin-1). Representative images are shown. The boxed region in the merged panel is enlarged and shown in the *Inset*. (Scale bar: 10 μm.) (*E*) Control or EphA2 shRNA-transduced HMVEC-d cells were subjected to Western blot analysis for the indicated phosphorylated (activated) signal molecules. The blots were stripped and reprobed for the respective total c-Cbl and myosin IIA with tubulin as a loading control. The levels of inhibition are indicated.

has been previously reported to be a signal for internalization upon ligand activation (31). Moreover, compared with control shRNA-transduced cells, in EphA2 shRNA-transduced cells, we observed a robust 60% statistically significant reduction in the induction of membrane blebs, which suggested a drastic reduction of macropinocytosis in KSHV-infected EphA2 shRNA-transduced cells (Fig. 6*B* and Fig. S7*A*).

To determine whether EphA2 played roles in the endocytic uptake of KSHV, we tracked the endosomal uptake of DiI-KSHV

(envelope labeled with DiI) in control and EphA2 shRNA-transduced HMVEC-d cells. Rab5 and its effectors have been shown to facilitate different endocytic pathways, including macropinocytosis-induced membrane ruffling (32). Rab5 signals were also recruited specifically to the internalized macropinosomes when induced by receptor tyrosine kinases (32–35). Hence, we determined the effect of EphA2 shRNA on the internalization of KSHV in Rab5-positive macropinosomes. At 10 min p.i., we observed that DiI-KSHV localized predominantly in Rab5-positive vesicles in control shRNA-transduced cells with an 82% colocalization frequency (Fig. 6*C* and Fig. S7*B*). In contrast, significantly reduced (22%) colocalization of virus with Rab5-positive macropinosomes was observed in EphA2 shRNA-transduced cells (Fig. 6*C* and Fig. S7*B*, *P* = 0.0004). Line-scan analysis of the enlarged cells clearly revealed the synchronized red signals (KSHV) within the green signal peaks (Rab5) in control shRNA cells but lacking in EphA2 shRNA-transduced cells (Fig. 6*D*). This result suggested that EphA2 was required for KSHV internalization in macropinosomes.

To further validate that EphA2 is involved in macropinocytosis of KSHV, we tracked the internalization of DiI-KSHV along with the macropinocytic marker dextran and EphA2. Compared with uninfected cells, we observed that EphA2 and dextran colocalized with internalized DiI-KSHV at 30 min p.i. (Fig. 6*E*). This observation indicated that DiI-KSHV was internalized along with the macropinocytic marker dextran and EphA2. These interesting observations clearly demonstrated that EphA2 played roles in macropinocytic entry of KSHV in HMVEC-d cells.

EphA2 Is Required for Productive Trafficking of KSHV Toward the Nucleus of Infected HMVEC-d Cells. EphA2 shRNA transduction inhibited KSHV entry by ~63% whereas >90% inhibition of KSHV gene expression was observed (Fig. 3). Hence, we next investigated the fate of viral particles entering target cells during knockdown of EphA2. We tracked the internalized DiI-KSHV particles in control and EphA2 shRNA-transduced cells with LysoTracker, a basophilic lysosomal marker. Compared with control shRNA-transduced cells, DiI-KSHV colocalized with Lyso-Tracker at 30 min p.i. in EphA2 shRNA-transduced cells (Fig. S7*C*). This result suggested that KSHV localized in lysosomal compartments in the absence of functional EphA2. Earlier, we have shown that accumulation of KSHV in lysosomal compartments leads to a nonproductive infection (12).

KSHV also required the activation of Rho-GTPases for efficient entry and cytosolic trafficking (7). Ephrins are known to modulate Rho-GTPases through a variety of signaling mechanisms (15, 36). To assess the effect of EphA2 in productive viral trafficking, we analyzed the activation of RhoA in control and EphA2 shRNA-transduced cells. Compared with control cells, we observed a strong reduction (>50%) of RhoA-GTP in EphA2 shRNA-transduced cells early during KSHV infection (Fig. 6*F*).

Impairment in productive viral trafficking leads to reduced nuclear delivery of viral DNA (3). To confirm whether EphA2 knockdown reduced the nuclear delivery of KSHV, we quantitated the amount of viral DNA trafficked to the nucleus in EphA2 shRNA-transduced cells by real-time DNA PCR for KSHV ORF73. Compared with control shRNA cells, we observed 54% and 92% inhibition in nuclear delivery of KSHV DNA by EphA2 shRNAs 3 and 4, respectively (Fig. 6*G*). This observation also explained the dramatic reduction in the ORF73 gene expression by EphA2 shRNAs because a minimal quantity of KSHV DNA trafficked to the nucleus in the absence of EphA2.

Discussion

Ephrin ligands and Eph receptor tyrosine kinases are crucial for migration, repulsion, and adhesion of cells during neuronal, vascular, and intestinal development (19). Both Ephrins and Eph receptors are membrane-bound proteins, which generate bidirectional signaling by interacting with each other. Signaling through Ephrins is
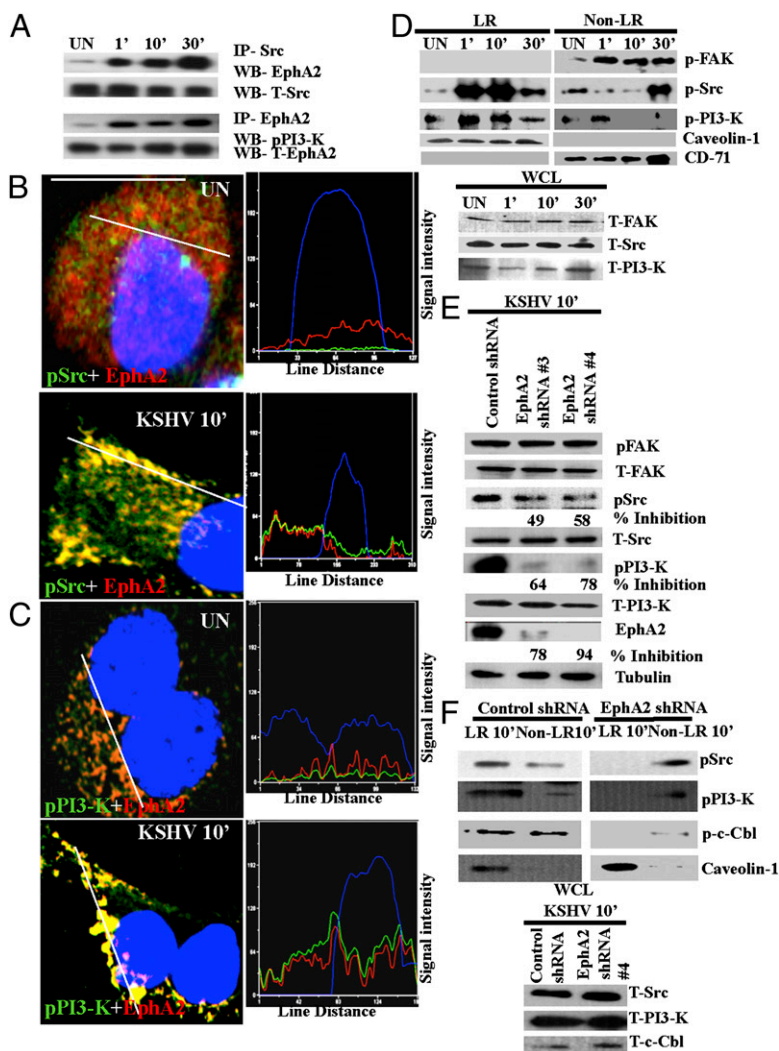
Fig. 5. EphA2 regulates the activation of KSHV-induced signal molecules during infection. (*A*) Serum-starved HMVEC-d cells were either left uninfected or KSHV infected for the indicated time points and immunoprecipitated with anti-Src or EphA2 antibodies and subjected to Western blot analyses for either EphA2 or pPI3-K. The blots were stripped and reprobed for the respective total proteins as indicated. (*B* and *C*) Serum-starved HMVEC-d cells were either mock or KSHV infected for 10 min. After washing, cells were processed for immunofluorescence microscopy using anti-pSrc (*B*) or pPI3-K (*C*) and EphA2 antibodies. They were subsequently stained with secondary antibodies conjugated with Alexa 488 or 594 and observed under an immunofluorescence microscope. Representative single-cell merged images with DAPI and line-scan signal intensity analysis are shown. (Scale bar: 10 μm). (*D*) One hundred fifty micrograms LR and non-LR fractions was analyzed by Western blots for phosphorylated signal molecules as indicated. Caveolin-1 and CD-71 are markers for LR and non-LR fractions, respectively. Twenty micrograms of whole-cell lysate (WCL) was subjected to Western blots for total protein levels. (*E*) Control or EphA2 shRNA-transduced HMVEC-d cells were subjected to Western blot analyses for the activated signal molecules (as indicated). The blots were stripped and reprobed for the respective total proteins and tubulin as a loading control. The levels of inhibition of activated signal molecules are indicated. (*F*) LR and non-LR fractions were isolated from control or EphA2 shRNA-transduced HMVEC-d cells infected with KSHV for 10 min. They were analyzed by Western blots for the indicated activated signal molecules. Caveolin-1 served as a marker for LR fractions. Twenty micrograms of WCL was subjected to Western blots for total protein levels.

called "reverse signaling," whereas signaling through Eph receptors is called "forward signaling" (19). The EphA2 receptor (also called Eck, Myk2, and Sek2), implicated in cancer, has been suggested as a therapeutic target for certain aggressive carcinomas because antibodies against the EphA2 receptor have been observed to inhibit growth of MDA-MB-231 breast tumor cells (36).

Our comprehensive analyses presented here have identified a unique role of EphA2 in coordinating and amplifying KSHV-induced signaling in LRs leading into KSHV internalization and gene expression in infected endothelial cells. Although EphB2 and EphA2 are reported to be the receptors for paramyxovirus (Henipavirus) and hepatitis C virus (HCV), respectively (28, 38, 39), the roles and mechanism by which Ephrin family members enhance these viral infections or affect infection-induced host cell signal modulation have not been studied before. We demonstrate that EphA2 acts as a master regulator of signaling induced during KSHV interactions with the entry receptors. Inhibition of EphA2 by shRNA(s), monoclonal antibodies, soluble receptor, or tyrosine kinase inhibitor cumulatively reveals an important role for EphA2 in productive KSHV entry into endothelial cells.

Evidence from the current study indicates that EphA2 is predominantly an LR partitioned molecule, which is consistent with a previous report where EphR-Eph ligand crosstalk occurring in lipid rafts was shown (40). In addition, the presence of Ephrins in lipid rafts has been shown to be crucial for raft signaling regulation events involving integrins (23). The observed selective c-Cbl–mediated KSHV–receptor translocation into LRs early during infection has probably evolved to interact with EphA2 in LRs, which is subsequently coupled to the formation of an integrin (α3β1 and αVβ3)-c-Cbl–EphA2 complex, the critical determinant of productive KSHV macropinocytosis. Because KSHV-induced Src and PI3-K activation still occurred in the non-LR portion of the membranes in EphA2 shRNA-transduced cells (Fig. 5 *E* and *F*), this result indicated that interaction of KSHV with integrins and subsequent activation of FAK, Src, PI3-K, and c-Cbl in non-LRs preceded rapid KSHV translocation into LRs along with α3β1, αVβ3, and xCT leading into EphA2 interaction. This process is critical for further amplification of Src and PI3-K activity in the LRs of KSHV-infected cells. Mutual dependency of EphA2 and KSHV-induced signaling leading toward efficient entry is further supported by our data where KSHV entry was remarkably abrogated by the tyrosine kinase inhibitor dasatinib, which inhibits Src and EphA2 kinases.

In EphA2 shRNA-transducd cells, a minimal quantity of KSHV, presumably non-LR αVβ5 bound KSHV, also entered the target cells. However, this action is not productive as KSHV nuclear delivery was drastically reduced and KSHV was targeted to lysosomes. These studies clearly demonstrated that EphA2-coordinated signaling complex formation in LRs is critical for productive macropinocytic infection and the absence of such amplification leads into a nonproductive infection.
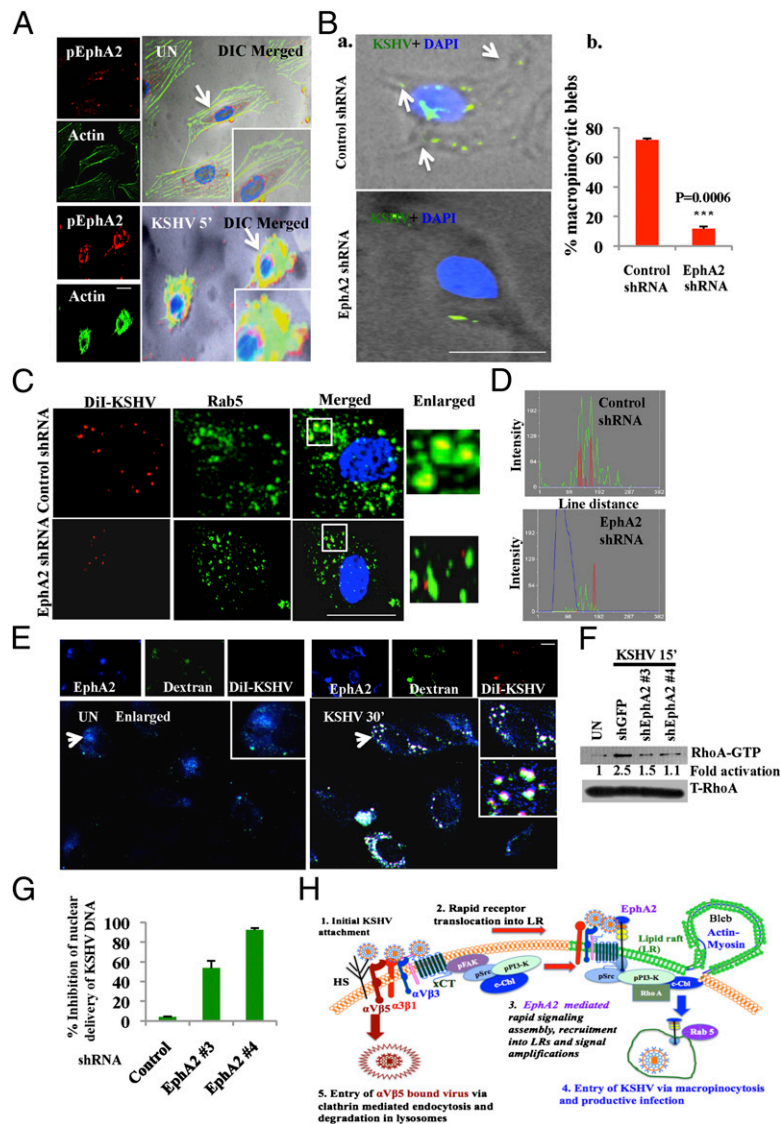
Fig. 6. EphA2 is required for productive endocytosis and trafficking of KSHV. (*A*) Serum-starved (8 h) HMVEC-d cells were either left uninfected or infected for 5 min with KSHV (10 DNA copies per cell), washed, and processed for immunofluorescence using rabbit anti-pEphA2 antibody, followed by anti-rabbit Alexa fluor 594 and phalloidin conjugated to Alexa 488. Representative DIC-merged images are shown. (*Right*) Arrows indicate EphA2 association with actin in the membrane ruffles. (*B*, *a*) Control and EphA2 shRNA-transduced HMVEC-d cells were infected with KSHV for 5 min and stained with anti-KSHV gpK8.1A monoclonal antibodies and DAPI. Representative DIC merged images are shown. Arrows indicate the regions of bleb formation in proximity to KSHV (green). (Scale bar: 10μm.) (*B*, *b*) Quantification of membrane blebs. The *P* value was calculated using a two-tailed Student's *t* test. (*C*) Serum-starved control or EphA2 shRNA-4–transduced HMVEC-d cells were infected with DiI-KSHV for 5 min, washed, and processed for immunofluorescence using Rab5 antibody. Boxed areas are enlarged and represented in the *Inset*. (Scale bar: 10 μm.) (*D*) Representation of line-scan signal intensity plots performed on the enlarged cell shown in *C*. (*E*) HMVEC-d cells were incubated with media containing FITC-Dextran with or without DiI-KSHV for 30 min at 37 °C. Cells were fixed and processed for immunofluorescence, using anti-EphA2 antibody followed by secondary antibody conjugated with Alexa 405. (Scale bar: 10 μm.) Arrows indicate the boxed areas that are enlarged and represented in the *Inset*. (*F*) Serum-starved HMVEC-d cells were infected with KSHV for 15 min. Cells were washed and RIPA lysates were collected. For RhoA activity analysis, 150 μg protein was incubated with Rhotekin RBD-GST beads for 2 h at 4 °C, followed by Western blot analysis for RhoA-GTP. The blot was stripped and blotted for total RhoA. (*G*) Control or EphA2 shRNA(s)-transduced HMVEC-d cells were infected with KSHV (10 DNA copies per cell) for 2 h. Postwashing, total DNA from nuclear extracts was prepared and normalized to 100 ng/5 μL. Real-time DNA-PCR for ORF73 was performed to detect viral DNA copies in the nucleus. Error bar represents mean ± SD of three experiments. (*H*) Model depicting the role of EphA2 in KSHV entry and infection: (*1*) KSHV's binding and interaction with heparan sulfate and integrins (α3β1, αVβ3, αVβ5) and x-CT initially occurs in non-LR regions. (*2*) This interaction is followed by c-Cbl–mediated rapid translocation of KSHV along with selective integrins (α3β1, αVβ3) and x-CT receptors into LRs. (*3*) This translocation promotes the association of EphA2 with translocated KSHV and integrins in the LRs. EphA2 coordinates the formation of an active signaling complex between integrins, c-Cbl and myosin IIA, thereby inducing macropinocytic blebs. To promote the necessary signaling stimulation required for macropinocytosis, EphA2 amplifies KSHV-induced pSrc, pPI3-K signaling, and the c-Cbl–myosin complex in the LRs. (*4*) Together, such complex signaling events trigger bleb formation, macropinocytosis, and internalization of KSHV into early macropinosomes that leads to productive trafficking of KSHV to the nucleus. (*5*) Non-LR αVβ5 bound viruses do not associate with EphA2 and are targeted toward a clathrin-dependent noninfectious lysosomal route.

EphA2 is known to be involved in integrin-associated signaling (41) and EphA2 is implicated in regulation of a variety of integrin signaling pathways (42). Ligand-induced EphA2 has been pre-

viously implicated in endocytosis and receptor clustering (43). Associations of pEphA2 with actins in membrane blebs as well as with dextran also support its role in macropinocytosis. Further-

more, c-Cbl and myosin-IIA are known regulators of KSHV macropinocytosis and their complex formation with EphA2 strongly advocates for a critical role of EphA2 during macropinocytosis. This outcome is supported by previous studies where c-Cbl mediated internalization of EphA2 (30). Although, c-Cbl drives the KSHV–receptor translocations into LRs, abrogation of sustained activation of c-Cbl and myosin-IIA and KSHV translocations by EphA2 shRNA clearly suggest that EphA2 augments c-Cbl–driven mechanisms in LRs and acts as a critical regulator of macropinocytosis.

Selective modulation of cellular signaling is crucial for endocytosis regulation (44). However, the molecule(s) involved in localized signaling assembly and thereby regulation of endocytosis in response to viral infection has not previously been identified. The lack of association of EphA2 with non-LR membrane-associated integrin αVβ5 and FAK and its association with KSHV-induced pSrc, pPI3-K, and c-Cbl signal molecules in LRs show that EphA2 regulates LR enrichment and selective amplification of signal molecules that control KSHV entry via macropinocytosis. Constitutive macropinocytosis and membrane ruffling induced in oncogene-transformed fibroblasts have been shown to be due to constant activation of Src, PI3-K, and PLC-C (45). Our earlier studies have shown that disruption of LRs can increase global pSrc activity and viral entry, but lead into nonproductive infection (9). Hence, localized and regulated amplification of Src-PI3-K signaling in LRs by EphA2 appears to be crucial for productive KSHV entry. It is possible that EphA2 regulates signal clustering in LRs to generate the mechanical force required for large macropinocytic vesicle formation and thereby facilitates KSHV internalization into target cells. Further studies are essential to decipher the downstream targets of EphA2 that play roles in the formation of macropinocytic vesicles.

Although microtubules and Rho-GTPases are known to regulate KSHV trafficking and entry (30), the current study reveals the dependency of Rho-GTPase on the upstream membrane protein EphA2 (7, 46). EphA2 also appears to be essential for Rab5 association with internalized KSHV in the early macropinosome and productive trafficking of KSHV. This observation is also supported by other studies where Eph-EphA2 complexes are implicated in different forms of endocytosis and cellular trafficking pathways (22). The factor(s) recognizing the EphA2-integrin-KSHV complex leading into macropinosome formation and sorting needs to be analyzed further.

The identification of receptor tyrosine kinases as an important host factor regulating KSHV infection advances knowledge of the molecular mechanisms and broad cellular requirements for assembled signal transduction, productive viral entry, and infection. Antibodies blocking EphA2, EphA2 inhibitors, and knockdown of EphA2 resulting in a reduction in KSHV-induced signaling, entry, and infection in endothelial cells suggest that EphA2 is a promising therapeutic target for controlling KSHV infection of endothelial cells and associated Kaposi's sarcoma.

Materials and Methods

Cells and Virus. Primary HMVEC-d cells (CC-2543; Clonetics) and HEK293T cells were grown as described before (11, 47). Induction of the KSHV lytic cycle in BCBL-1 cells, supernatant collection, and virus purification procedures were described previously (4). KSHV DNA was extracted and copies were quantitated by real-time DNA PCR, using primers amplifying the KSHV ORF73 gene as described previously (48). The lipophilic carbocyanine Dil-1,1'-dioctadecyl-3,3,3',3'-tetramethylindocarbocyanine perchlorate, [DiIC$_{18}$3], was used to label KSHV particles using methods described previously (12, 49).

Generation of EphA2 shRNA-Transduced Cells. We used five TRC human EphA2 shRNA-lentivirus constructs designed from the EphA2 sequence (GenBank accession no. NM_004431), which were obtained from Open Biosystems (RHS4533). Details are provided in *SI Materials and Methods*.

Plasmid and Transfections. Full-length EphA2-Myc–tagged plasmids were a kind gift from Horonari Katoh (Laboratory of Molecular Neurobiology, Graduate School of Biostudies, Kyoto University, Kyoto, Japan) (15). HEK293T cells were transiently transfected using calcium phosphate as described previously (47). See *SI Materials and Methods* for details.

Antibodies and Reagents. See *SI Materials and Methods*.

Immunoprecipitation. Two hundred micrograms of cell lysates were incubated for 2 h with immunoprecipitating antibody at 4 °C, and the resulting immune complexes were captured by protein G-Sepharose and analyzed by Western blots, using specific detection antibodies.

Western Blotting. Cells were lysed in RIPA buffer containing a protease inhibitor mixture (Sigma) and incubated on a rocker at 4 °C for 15 min. Lysates were normalized to equal amounts of protein, separated by 10% SDS/PAGE, transferred to nitrocellulose, and probed with the indicated primary antibodies. Detection was by incubation with species-specific HRP-conjugated secondary antibodies. Immunoreactive bands were visualized by enhanced chemiluminescence (Pierce). The bands were scanned and quantitated using FluorChemFC2 and an Alpha-Imager (Alpha Innotech).

Lipid Raft Extraction and Characterization. Lipid raft extraction was performed following the manufacturer's protocol for the caveolae/rafts isolation kit (Sigma) on the basis of nondetergent density gradient extraction of lipid rafts (50). See *SI Materials and Methods* for details.

Mass Spectrometry. Serum-starved (8 h) HMVEC-d cells were either mock or KSHV (10 DNA copies per cell) infected for 5 min. LR and nonlipid raft (non-LR) fractions were isolated. Two hundred micrograms protein from LR and non-LR fractions was immunoprecipitated with mouse anti-α3β1 and control antibody. Immunoprecipitates were separated by 10% SDS/PAGE and the bands specific for α3β1 immunoprecipitates were analyzed by mass spectrometry, using LC-electrospray ionization (ESI)-MS methods at the Midwest Proteome Center, Rosalind Franklin University of Medicine and Sciences.

Measurement of KSHV Binding, Entry, and Nuclear Delivery by Real-Time DNA PCR. HMVEC-d cells were infected with KSHV (10 DNA copies per cell) at 4 °C (binding) or 37 °C (entry and nuclear delivery) for 1 h. Details are provided in *SI Materials and Methods*.

Measurement of KSHV Gene Expression by Real-Time Reverse Transcription (RT-PCR). Total RNA was prepared from infected or uninfected cells, using an RNeasy kit (QIAGEN) as described previously, and viral gene expression was determined (48). See *SI Materials and Methods* for details.

Measurement of KSHV Infection in the Presence of Soluble EphA2. Ten DNA copies per cell of KSHV were preincubated with 10 μg/ml recombinant soluble EphA2 (Sol-EphA2) (R&D Systems) for 1 h at 37 °C. HMVEC-d cells were infected with unincubated or Sol-EphA2 incubated KSHV for 1 h at 37 °C. KSHV DNA binding, entry, and gene expression were measured as described in *SI Materials and Methods*.

Measurement of KSHV Entry in the Presence of Antibodies Against EphA2. HMVEC-d cells were incubated with 10 μg/mL rabbit mAbs against EphA2, EphB2, or control IgG for 1 h at 4 °C. After washing, cells were infected with 10 DNA copies per cell of KSHV for 1 h at 37 °C. KSHV entry was determined as described in *SI Materials and Methods*.

RhoA Activation Analysis. One hundred fifty micrograms of cell lysates was incubated with Rhotekin RBD-GST beads for 2 h. The resulting bound Rho-GTP complexes were analyzed by a Western blot for RhoA.

Immunofluorescence Microscopy. See *SI Materials and Methods* for details.

Quantification of Macropinocytic Blebs. Determination of blebs in KSHV-infected cells was performed as described previously (11) (*SI Materials and Methods*).

1. Chang Y, et al. (1994) Identification of herpesvirus-like DNA sequences in AIDS-associated Kaposi's sarcoma. *Science* 266:1865–1869.
2. Ganem D (2007) Kaposi's sarcoma-associated herpesvirus. *Fields Virology*, eds Knipe DM, et al. (Lippincott Williams & Wilkins, Philadelphia), 5th Ed, Vol 2, pp 2875–2888.
3. Chandran B (2010) Early events in Kaposi's sarcoma-associated herpesvirus infection of target cells. *J Virol* 84:2188–2199.
4. Akula SM, Pramod NP, Wang FZ, Chandran B (2002) Integrin alpha3beta1 (CD 49c/29) is a cellular receptor for Kaposi's sarcoma-associated herpesvirus (KSHV/HHV-8) entry into the target cells. *Cell* 108:407–419.
5. Akula SM, et al. (2003) Kaposi's sarcoma-associated herpesvirus (human herpesvirus 8) infection of human fibroblast cells occurs through endocytosis. *J Virol* 77:7978–7990.
6. Naranatt PP, Akula SM, Zien CA, Krishnan HH, Chandran B (2003) Kaposi's sarcoma-associated herpesvirus induces the phosphatidylinositol 3-kinase-PKC-zeta-MEK-ERK signaling pathway in target cells early during infection: Implications for infectivity. *J Virol* 77:1524–1539.
7. Veettil MV, et al. (2006) RhoA-GTPase facilitates entry of Kaposi's sarcoma-associated herpesvirus into adherent target cells in a Src-dependent manner. *J Virol* 80:11432–11446.
8. Sadagopan S, et al. (2007) Kaposi's sarcoma-associated herpesvirus induces sustained NF-kappaB activation during de novo infection of primary human dermal microvascular endothelial cells that is essential for viral gene expression. *J Virol* 81:3949–3968.
9. Raghu H, et al. (2007) Lipid rafts of primary endothelial cells are essential for Kaposi's sarcoma-associated herpesvirus/human herpesvirus 8-induced phosphatidylinositol 3-kinase and RhoA-GTPases critical for microtubule dynamics and nuclear delivery of viral DNA but dispensable for binding and entry. *J Virol* 81:7941–7959.
10. Mercer J, Helenius A (2009) Virus entry by macropinocytosis. *Nat Cell Biol* 11:510–520.
11. Valiya Veettil M, Sadagopan S, Kerur N, Chakraborty S, Chandran B (2010) Interaction of c-Cbl with myosin IIA regulates Bleb associated macropinocytosis of Kaposi's sarcoma-associated herpesvirus. *PLoS Pathog* 6:e1001238.
12. Chakraborty S, ValiyaVeettil M, Sadagopan S, Paudel N, Chandran B (2011) c-Cbl-mediated selective virus-receptor translocations into lipid rafts regulate productive Kaposi's sarcoma-associated herpesvirus infection in endothelial cells. *J Virol* 85:12410–12430.
13. Himanen JP, et al. (2009) Ligand recognition by A-class Eph receptors: Crystal structures of the EphA2 ligand-binding domain and the EphA2/ephrin-A1 complex. *EMBO Rep* 10:722–728.
14. Pasquale EB (2008) Eph-ephrin bidirectional signaling in physiology and disease. *Cell* 133:38–52.
15. Hiramoto-Yamaki N, et al. (2010) Ephexin4 and EphA2 mediate cell migration through a RhoG-dependent mechanism. *J Cell Biol* 190:461–477.
16. Egea J, Klein R (2007) Bidirectional Eph-ephrin signaling during axon guidance. *Trends Cell Biol* 17:230–238.
17. Himanen JP, Saha N, Nikolov DB (2007) Cell-cell signaling via Eph receptors and ephrins. *Curr Opin Cell Biol* 19:534–542.
18. Miao H, et al. (2005) Inhibition of integrin-mediated cell adhesion but not directional cell migration requires catalytic activity of EphB3 receptor tyrosine kinase. Role of Rho family small GTPases. *J Biol Chem* 280:923–932.
19. Pasquale EB (2005) Eph receptor signalling casts a wide net on cell behaviour. *Nat Rev Mol Cell Biol* 6:462–475.
20. Brantley-Sieders DM, et al. (2004) EphA2 receptor tyrosine kinase regulates endothelial cell migration and vascular assembly through phosphoinositide 3-kinase-mediated Rac1 GTPase activation. *J Cell Sci* 117:2037–2049.
21. Deroanne C, Vouret-Craviari V, Wang B, Pouysségur J (2003) EphrinA1 inactivates integrin-mediated vascular smooth muscle cell spreading via the Rac/PAK pathway. *J Cell Sci* 116:1367–1376.
22. Pitulescu ME, Adams RH (2010) Eph/ephrin molecules—a hub for signaling and endocytosis. *Genes Dev* 24:2480–2492.
23. Huai J, Drescher U (2001) An ephrin-A-dependent signaling pathway controls integrin function and is linked to the tyrosine phosphorylation of a 120-kDa protein. *J Biol Chem* 276:6689–6694.
24. Gauthier LR, Robbins SM (2003) Ephrin signaling: One raft to rule them all? One raft to sort them? One raft to spread their call and in signaling bind them? *Life Sci* 74:207–216.
25. Kullander K, Klein R (2002) Mechanisms and functions of Eph and ephrin signalling. *Nat Rev Mol Cell Biol* 3:475–486.
26. Chen J, Zhuang G, Frieden L, Debinski W (2008) Eph receptors and Ephrins in cancer: Common themes and controversies. *Cancer Res* 68:10031–10033.
27. Davy A, Robbins SM (2000) Ephrin-A5 modulates cell adhesion and morphology in an integrin-dependent manner. *EMBO J* 19:5396–5405.
28. Lupberger J, et al. (2011) EGFR and EphA2 are host factors for hepatitis C virus entry and possible targets for antiviral therapy. *Nat Med* 17:589–595.
29. Schmidt MH, Dikic I (2005) The Cbl interactome and its functions. *Nat Rev Mol Cell Biol* 6:907–918.
30. Raghu H, Sharma-Walia N, Veettil MV, Sadagopan S, Chandran B (2009) Kaposi's sarcoma-associated herpesvirus utilizes an actin polymerization-dependent macropinocytic pathway to enter human dermal microvascular endothelial and human umbilical vein endothelial cells. *J Virol* 83:4895–4911.
31. Walker-Daniels J, Riese DJ, 2nd, Kinch MS (2002) c-Cbl-dependent EphA2 protein degradation is induced by ligand binding. *Mol Cancer Res* 1:79–87.
32. Schnatwinkel C, et al. (2004) The Rab5 effector Rabankyrin-5 regulates and coordinates different endocytic mechanisms. *PLoS Biol* 2:E261.
33. Coyne CB, Shen L, Turner JR, Bergelson JM (2007) Coxsackievirus entry across epithelial tight junctions requires occludin and the small GTPases Rab34 and Rab5. *Cell Host Microbe* 2:181–192.
34. Sun P, et al. (2003) Small GTPase Rah/Rab34 is associated with membrane ruffles and macropinosomes and promotes macropinosome formation. *J Biol Chem* 278:4063–4071.
35. Lanzetti L, et al. (2007) Regulation of the Rab5 GTPase-activating protein RN-tre by the dual specificity phosphatase Cdc14A in human cells. *J Biol Chem* 282:15258–15270.
36. Brantley-Sieders DM, et al. (2008) The receptor tyrosine kinase EphA2 promotes mammary adenocarcinoma tumorigenesis and metastatic progression in mice by amplifying ErbB2 signaling. *J Clin Invest* 118:64–78.
37. Carles-Kinch K, Kilpatrick KE, Stewart JC, Kinch MS (2002) Antibody targeting of the EphA2 tyrosine kinase inhibits malignant cell behavior. *Cancer Res* 62:2840–2847.
38. Bonaparte MI, et al. (2005) Ephrin-B2 ligand is a functional receptor for Hendra virus and Nipah virus. *Proc Natl Acad Sci USA* 102:10652–10657.
39. Negrete OA, et al. (2005) EphrinB2 is the entry receptor for Nipah virus, an emergent deadly paramyxovirus. *Nature* 436:401–405.
40. Murai KK, Pasquale EB (2004) Eph receptors, ephrins, and synaptic function. *Neuroscientist* 10:304–314.
41. Parri M, et al. (2007) EphrinA1 activates a Src/focal adhesion kinase-mediated motility response leading to rho-dependent actino/myosin contractility. *J Biol Chem* 282:19619–19628.
42. Miao H, Burnett E, Kinch M, Simon E, Wang B (2000) Activation of EphA2 kinase suppresses integrin function and causes focal-adhesion-kinase dephosphorylation. *Nat Cell Biol* 2:62–69.
43. Zhuang G, Hunter S, Hwang Y, Chen J (2007) Regulation of EphA2 receptor endocytosis by SHIP2 lipid phosphatase via phosphatidylinositol 3-Kinase-dependent Rac1 activation. *J Biol Chem* 282:2683–2694.
44. Sorkin A, von Zastrow M (2009) Endocytosis and signalling: Intertwining molecular networks. *Nat Rev Mol Cell Biol* 10:609–622.
45. Amyere M, et al. (2000) Constitutive macropinocytosis in oncogene-transformed fibroblasts depends on sequential permanent activation of phosphoinositide 3-kinase and phospholipase C. *Mol Biol Cell* 11:3453–3467.
46. Naranatt PP, Krishnan HH, Smith MS, Chandran B (2005) Kaposi's sarcoma-associated herpesvirus modulates microtubule dynamics via RhoA-GTP-diaphanous 2 signaling and utilizes the dynein motors to deliver its DNA to the nucleus. *J Virol* 79:1191–1206.
47. Bottero V, et al. (2009) Kaposi sarcoma-associated herpes virus (KSHV) G protein-coupled receptor (vGPCR) activates the ORF50 lytic switch promoter: A potential positive feedback loop for sustained ORF50 gene expression. *Virology* 392:34–51.
48. Krishnan HH, et al. (2004) Concurrent expression of latent and a limited number of lytic genes with immune modulation and antiapoptotic function by Kaposi's sarcoma-associated herpesvirus early during infection of primary endothelial and fibroblast cells and subsequent decline of lytic gene expression. *J Virol* 78:3601–3620.
49. Le Blanc I, et al. (2005) Endosome-to-cytosol transport of viral nucleocapsids. *Nat Cell Biol* 7:653–664.
50. Song KS, et al. (1996) Co-purification and direct interaction of Ras with caveolin, an integral membrane protein of caveolae microdomains. Detergent-free purification of caveolae microdomains. *J Biol Chem* 271:9690–9697.